

Effect of static and dynamic disorder on electronic transport of $R\text{Co}_2$ compounds: a study of $\text{Ho}(\text{Al}_x\text{Co}_{1-x})_2$ alloys

A. T. Burkov

A.F.Ioffe Physico-Technical Institute, Russian Academy of Sciences, Sankt-Petersburg 194021, Russia.

E. Bauer, E. Gratz

*Institute of Experimental Physics, Vienna Technical University,
Wiedner Hauptstrasse 8-10, A-1040 Vienna, Austria.*

R. Resel

Institute of Solid State Physics, Graz University of Technology, Petergasse 16, A-8010 Graz, Austria

T. Nakama, K. Yagasaki

Department of Physics, College of Science, University of the Ryukyus, Okinawa 903-0213, Japan.

(Dated: October 26, 2018)

We present experimental results on thermoelectric power (S) and electrical resistivity (ρ) of pseudobinary alloys $\text{Ho}(\text{Al}_x\text{Co}_{1-x})_2$ ($0 \leq x \leq 0.1$), in the temperature range 4.2 K to 300 K. The work focuses on the effects of static (induced by alloying) and dynamic (induced by temperature) disorder on the magnetic state and electronic transport in a metallic system with itinerant metamagnetic instability. Spatial fluctuations of the local magnetic susceptibility in the alloys lead to the development of a partially ordered magnetic ground state of the itinerant $3d$ electron system. This results in a strong increase of the residual resistivity and a suppression of the temperature-dependent resistivity. Thermopower exhibits a complex temperature variation in both the magnetically ordered and in the paramagnetic state. This complex temperature variation is attributed to the electronic density of states features in vicinity of Fermi energy and to the interplay of magnetic and impurity scattering. Our results indicate that the magnetic enhancement of the Co $3d$ band in $R\text{Co}_2$ -based alloys upon a substitution of Co by non-magnetic elements is mainly related to a progressive localization of the Co $3d$ electrons caused by disorder. We show that the magnitude of the resistivity jump at the Curie temperature for $R\text{Co}_2$ compounds exhibiting a first order phase transition is a non-monotonic function of the Curie temperature due to a saturation of the $3d$ -band spin fluctuation magnitude at high temperatures.

PACS numbers: 71.27.+a, 72.15.Gd, 72.15.Jf, 75.10.Lp, 75.30.Kz

HoCo_2 belongs to the family of intermetallic $R\text{Co}_2$ cubic Laves phases (R stands for rare earth elements) which are well known for their outstanding magnetic properties associated with itinerant $3d$ electron subsystem^{1,2,3}. Long-range magnetic order of the $3d$ electron subsystem of paramagnetic YCo_2 and LuCo_2 can be induced by external magnetic field exceeding a certain critical value B_c . This critical field was found to be about 70 T for YCo_2 ⁴ and about 77 T for LuCo_2 ⁵. Partial replacement of cobalt by aluminium leads to a decrease of B_c and to the appearance of weak itinerant ferromagnetism in $\text{Y}(\text{Al}_x\text{Co}_{1-x})_2$ for $x > 0.12$ ^{6,7}. In the case of magnetic $R\text{Co}_2$ compounds, long-range magnetic order of the $3d$ electron subsystem is induced by ordering of the localized magnetic moments of the rare earths. A substitution of Al on Co-sites of the magnetic $R\text{Co}_2$ compounds, results in a considerable increase of the Curie temperature⁸.

This behavior was interpreted within the framework of the itinerant magnetism by an increase of the density of states (DOS) at the Fermi level as Co is replaced by Al. However, the mechanism, responsible for the increase of DOS at the Fermi level, remains obscure. Mainly two scenarios have been proposed: in the first, DOS increases due to de-population of $3d$ -Co band when Co is replaced

by Al^{6,9}; in the second, the DOS increase is caused by a narrowing of the $3d$ band due to an expansion of the crystal lattice in the alloys^{7,10}.

In the present work we use the temperature dependent thermopower $S(T)$ to study the mechanism of the DOS enhancement in Al-substituted $R\text{Co}_2$ compounds. It has been shown that $S(T)$ high-temperature minimum, observed in $S(T)$ of nearly all $R\text{Co}_2$ compounds in a range from 150 K to 400 K, is associated with a sharp peak in the density of states related mainly to the Co $3d$ -electron density¹¹. Particularly, it was shown that the temperature T_{\min} , at which the thermopower has this minimum, is a measure of the DOS peak width^{3,12}.

Another unsolved problem, related to metamagnetism and charge transport in $R\text{Co}_2$ compounds is the different order of the phase transition at Curie temperature (T_c) and a non-monotonic variation of the resistivity jump ($\Delta\rho$) at T_c . Among the $R\text{Co}_2$ compounds, ErCo_2 , HoCo_2 and DyCo_2 undergo a first order phase transition at T_c , whereas it is generally accepted that in TbCo_2 , GdCo_2 , TmCo_2 and SmCo_2 the magnetic ordering is via second order transition. The kind of the phase transition at T_c in PrCo_2 and NdCo_2 has been a subject of recent discussion^{13,14,15,16}. In this context the $\text{Ho}(\text{Al}_x\text{Co}_{1-x})_2$

alloys are proper materials to study, since this alloy system includes compounds with both, first order, and second order transition at T_c .

I. EXPERIMENTAL PROCEDURES

The samples of $\text{Ho}(\text{Co}_{1-x}\text{Al}_x)_2$ alloys were prepared from pure components by melting in an induction furnace under a protective Ar atmosphere and were subsequently annealed in vacuum at 1100 K for about one week. The X-ray analysis showed no traces of impurity phases.

A four-probe dc method was used for the electrical resistivity measurements; for the thermopower measurements a differential method was applied. Typical size of the samples was about $1 \times 1 \times 10 \text{ mm}^3$. The estimated error in the absolute value of the electrical resistivity is $\pm 10\%$. This is mainly due to uncertainty in the sample geometry which is closely related to the mechanical quality of the samples. The thermopower was measured with an accuracy of $\pm 0.2 \mu\text{VK}^{-1}$.

II. EXPERIMENTAL RESULTS.

The resistivity temperature dependencies are depicted in Figure 1. The residual resistivity, shown in the inset, rapidly increases with Al content. Simultaneously, the temperature dependent part of the resistivity decreases, so that the high temperature total resistivity shows a comparatively small change with composition. Room temperature values are in the range of 130 to $150 \mu\Omega\text{cm}$. The Curie temperature is marked by an abrupt change

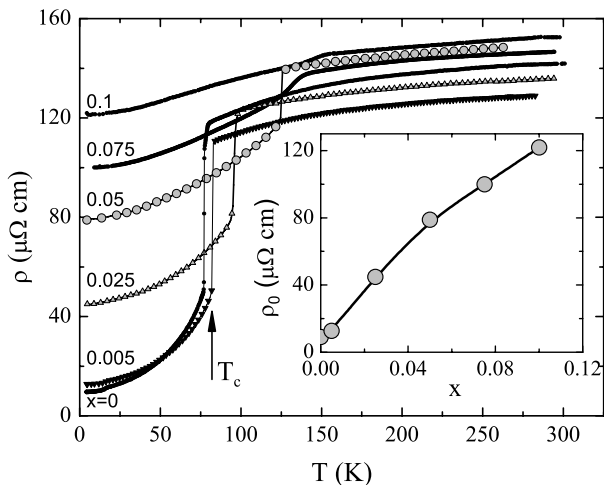


FIG. 1: Temperature dependent resistivity of $\text{Ho}(\text{Co}_{1-x}\text{Al}_x)_2$ for various Al concentrations. The inset shows the composition dependence of the residual resistivity, measured at 4.2 K.

of the resistivity of the samples with $x=0, 0.005, 0.025,$ and 0.05 , whereas samples with $x=0.075$ and 0.1 clearly show a second order-like variation of the resistivity at T_c .

Data of Fig. 1 indicate that the boundary between first-order and second-order transitions is between $x=0.05$ and $x=0.075$. These results agree with the data of Duc et al.¹⁷.

Figure 2 presents experimental results for the thermopower from 5 K to 300 K. Dramatic changes of $S(T)$ with the alloy composition are clearly seen in both, the paramagnetic and in the magnetically ordered state of the alloys. At high temperatures the $S(T)$ minimum temperature T_{min} , observable for pure HoCo_2 at 250 K, and the absolute $S(T)$ values decrease with increasing Al content. In the low temperature region, ($T < T_c$), $S(T)$ is also strongly dependent on the Al-content.

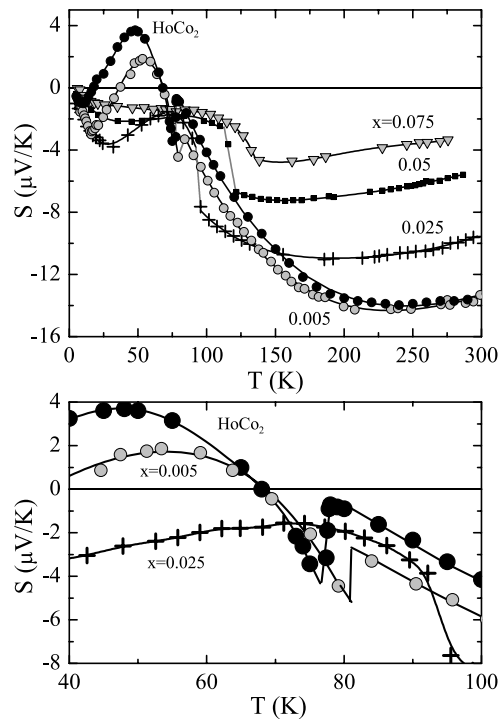


FIG. 2: Temperature dependent thermopower of $\text{Ho}(\text{Co}_{1-x}\text{Al}_x)_2$. The lower panel shows $S(T)$ of the $x = 0, x = 0.005$ and $x = 0.025$ alloys in a vicinity of Curie temperature.

At the lowest temperatures all compounds exhibit a minimum with negative $S(T)$ values; its temperature gradually increases with Al concentration. The $S(T)$ minimum, as well as the following maximum, become suppressed for $x=0.05$ and they almost disappear for $x=0.075$. The Curie temperatures are associated with the discontinuous changes of $S(T)$ for $x=0, 0.005, 0.025$, whereas the sample with $x=0.075$ clearly shows a second order-like variation of the thermopower at T_c .

III. DISCUSSION.

A. Variation of the 3d-DOS upon substitution of cobalt by non-magnetic elements.

The temperature variation of the thermopower in the paramagnetic temperature region can be understood within the model proposed in^{3,12,18}. Calculations of the density of states, $N(\varepsilon)$ for YCo_2 ^{19,20,21,22} revealed the Fermi level, ε_F , lying near a sharp peak of DOS, primarily composed of 3d states of Co (Figure 3). Since

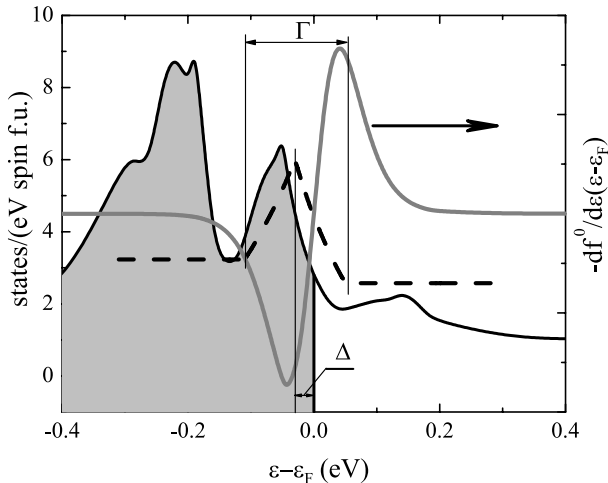


FIG. 3: DOS of $R\text{Co}_2$ compounds in a vicinity of the Fermi level (solid line)²⁰. The gray line shows $-df^0/d\varepsilon(\varepsilon - \varepsilon_F)$ at $T=300$ K (f^0 is Fermi distribution function) to indicate the energy region important for transport properties. The broken line is the model state density, used for thermopower calculations. Γ is the width of the model DOS peak, Δ - is the distance from Fermi level to the center of the peak.

Co is present in all $R\text{Co}_2$ compounds, it is assumed, that $N(\varepsilon)$ has the same general features throughout the $R\text{Co}_2$ series.

It has been shown that the high-temperature minimum, observed in $S(T)$ of nearly all $R\text{Co}_2$ compounds (with the exception of GdCo_2 , DyCo_2 , and SmCo_2 where T_{\min} falls into the temperature range where these compounds order magnetically), is associated with the 3d peak of the DOS, T_{\min} being the measure of the peak width^{3,12}.

Since the width of an itinerant electronic band depends on the extent of the corresponding atomic orbital overlapping, one should expect that the 3d peak width increases when the lattice parameter decreases. The lattice parameter within $R\text{Co}_2$ compounds reveals considerable variation, being smallest for ScCo_2 and largest for NdCo_2 . This implies that the 3d DOS peak width is largest in case of ScCo_2 and smallest for NdCo_2 with corresponding variation of T_{\min} . This assumption has been confirmed by a good correlation between T_{\min} and the lattice constants of the $R\text{Co}_2$ compounds³. Figure 4a reproduces, in part, this correlation.

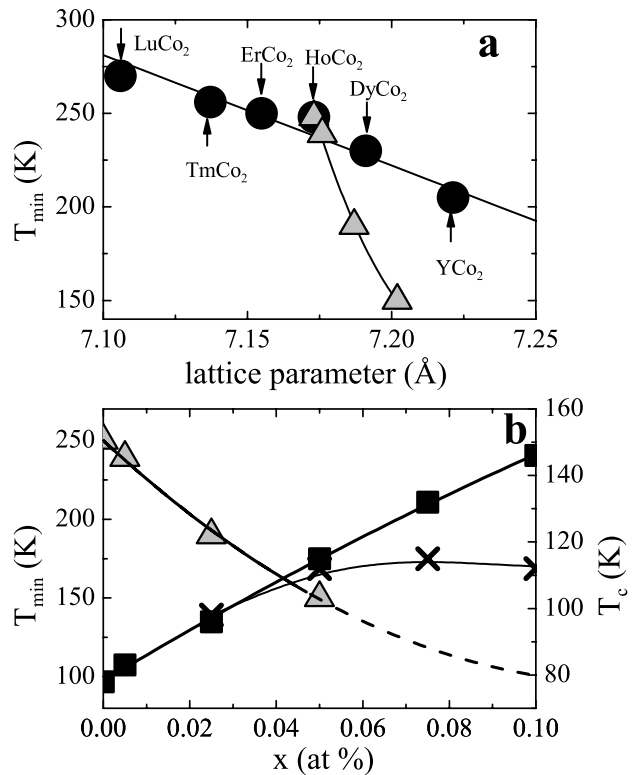


FIG. 4: **a.** Dependence of T_{\min} against lattice parameter for $R\text{Co}_2$ compounds (\bullet - data from³). The triangles show this work results for $\text{Ho}(\text{Co}_{1-x}\text{Al}_x)_2$ alloys. **b.** T_{\min} (triangles) and Curie temperature T_c (\blacksquare) against composition for $\text{Ho}(\text{Co}_{1-x}\text{Al}_x)_2$. \times - T_c against composition for $\text{Ho}(\text{Co}_{1-x}\text{Si}_x)_2$ alloys according to Ref.²³.

The decrease of T_{\min} with increasing Al content in $\text{Ho}(\text{Co}_{1-x}\text{Al}_x)_2$ alloys (Fig. 4b) indicates a narrowing of the 3d DOS peak. Partially this narrowing can be connected with the increase of the lattice parameter in the alloys. However, the expansion of the crystal lattice is insufficient to entirely account for the narrowing of the DOS peak and the observed increase of the Curie temperature. If the decrease of T_{\min} was related only to the lattice expansion, then one would expect that T_{\min} in the alloys decreases roughly at the same rate as in pure $R\text{Co}_2$ compounds. However, the results for $\text{Ho}(\text{Co}_{1-x}\text{Al}_x)_2$ reveal a much stronger dependence of T_{\min} on the lattice parameter (Fig.4a), implying that some additional factor is responsible for the narrowing of the peak width and increase of T_c .

Literature results on $\text{Y}_{1-t}\text{Lu}_t(\text{Co}_{1-x}\text{Al}_x)_2$ ²⁸ alloys with invariable lattice parameter show, that at small x (up to about $x=0.06-0.1$) the critical field for metamagnetic transition in these alloys decreases at the same rate as in $\text{Lu}(\text{Co}_{1-x}\text{M}_x)_2$ ($M = \text{Ga}, \text{Sn}, \text{Al}$)^{24,25} and $\text{Y}(\text{Co}_{1-x}\text{Al}_x)_2$ ^{26,27} alloys, where lattice parameter varies considerably. Similarly, in $\text{Ho}(\text{Co}_{1-x}\text{Si}_x)_2$ diluted alloys²³ with invariable lattice parameter and in $\text{Ho}(\text{Co}_{1-x}\text{Al}_x)_2$ alloys T_c increases with x at the same

rate, see Fig. 4b. This indicates, in agreement with our results, that lattice expansion can not be the main cause for the magnetic enhancement of the alloys. On the other hand, the $3d$ band de-population model also can not explain these results since the substituting elements have different configurations of the outer electronic shells.

The results show that the mechanism, which causes the decrease of B_c in non-magnetic compounds (or increase of T_c in the magnetic ones) does depend at small x neither on the type of substituting element nor on the lattice expansion. What all above mentioned alloys have in common, is disorder within the Co-sublattice due the substitution of Co by other elements. We therefore conclude, that the principal reason for the narrowing of the $3d$ band in $\text{Ho}(\text{Co}_{1-x}\text{Al}_x)_2$ for low Al contents, is the increasing localization of the $3d$ electrons caused by disorder within Co-sublattice. Experimental results on transport in $\text{Y}(\text{Co}_{1-x}\text{Al}_x)_2$ alloys has led us to a similar conclusion²⁹. A different situation takes place when the impurity element has unfilled $3d$ -shell, like Ni and Fe, in that case the effects of the change of $3d$ electron concentration play a dominant role³⁰.

Of course, one can not exclude a change of the $3d$ electron concentration upon the Co-substitution in $\text{Ho}(\text{Co}_{1-x}\text{Al}_x)_2$. Moreover, the decrease of $S(T)$ values in the paramagnetic temperature region, as will be demonstrated later, implies such a change. It also follows from literature that the behavior of $\text{Y}(\text{Co}_{1-x}\text{M}_x)_2$ alloys at large x (above about 0.1), such as the stabilization of a ferromagnetic ground state, depends on the kind of substituting elements, suggesting a hybridization of s - p and $3d$ states. However, our analysis shows that the change of the $3d$ electron concentration does not play major role in magnetic enhancement of diluted alloys.

To summarize this part, our experimental results on transport properties of $\text{Ho}(\text{Co}_{1-x}\text{Al}_x)_2$ alloys and analysis of the results, reported in the literature, led us to the conclusion that the principal mechanism, responsible for the increase of T_c in magnetic alloys, or a decrease of B_c in paramagnetic alloys, is the narrowing of the $3d$ DOS peak due to localization of Co $3d$ electron states, induced by disorder in Co sublattice of the alloys.

B. Electrical resistivity.

The rapid increase of the residual resistivity and the modest variation of high temperature resistivity with Al content are the most characteristic features observed in the resistivity of the alloys. The temperature dependent part of the resistivity systematically decreases with x as it is shown in Fig. 5. We should note that such behavior is common for many $R\text{Co}_2$ -based alloys^{23,26,31,32,33,34,35}, which include both, $R(\text{Co}_{1-x}\text{M}_x)_2$ and $\text{Y}_{1-x}\text{R}_x\text{Co}_2$ systems. However, there has been no commonly accepted model, able to account for the observed variation of the temperature dependent resistivity. The independence of the phenomenon on the constituents of the alloys implies

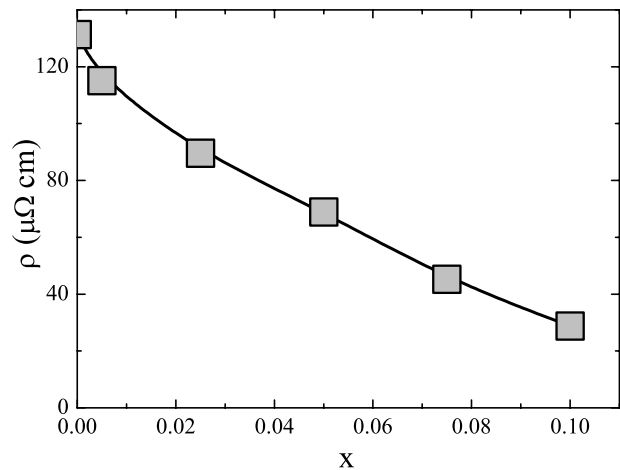


FIG. 5: Temperature – induced part of resistivity ($\rho(250) - \rho(4.2)$) of $\text{Ho}(\text{Co}_{1-x}\text{Al}_x)_2$ alloys.

a common mechanism. As in the case of the above discussed Co-localization, disorder and metamagnetism of the magnetic Co subsystem are the natural candidates. Baranov et al.^{36,37} were probably the first to emphasize the important role, which disorder can play in $R\text{Co}_2$ -based alloys. In a certain range of alloy composition, $3d$ magnetic subsystem can be in "partially" ordered ground state, i.e. in the alloy there are spatial regions with high and low $3d$ magnetization. This static magnetic disorder originates from a combination of fluctuating exchange field (in $(\text{Y}_{1-x}\text{R}_x)\text{Co}_2$ alloys), or fluctuating local susceptibility (in $R(\text{Co}_{1-x}\text{M}_x)_2$ alloys), and of the metamagnetism of $3d$ electron system. Scattering of conduction electrons of this static magnetic disorder gives contribution to the alloy resistivity, which is comparable to the high temperature limit of $3d$ spin fluctuation (SF) resistivity (the resistivity due to scattering on dynamic, i.e. temperature-induced, fluctuations of local $3d$ magnetization) in $R\text{Co}_2$ compounds³⁸. The static magnetic disorder can be viewed as "frozen" SF. When temperature increases this frozen disorder melts and is replaced by the dynamic disorder. Since the corresponding contributions to resistivity are of similar magnitude, the temperature variation of the total resistivity is considerably reduced.

Figure 6 shows the resistivity of $\text{Ho}(\text{Co}_{1-x}\text{Al}_x)_2$, DyCo_2 and TbCo_2 ³⁹, normalized to its value at $T=300$ K, plotted against T/T_{\min} to account for the different width of the $3d$ band. Since for the $\text{Ho}(\text{Co}_{1-x}\text{Al}_x)_2$ with $x > 0.075$ the high-temperature minimum in $S(T)$ is not observable due to the high T_c , we use an interpolation of $T_{\min}(x)$, as it is shown in Fig. 4b by the broken line, to obtain T_{\min} of these alloys.

The other two interesting features of the resistivity can be seen from Figure 6:

1. The kind of the phase transition at Curie point is changed from first to second order around $T_c=T_{\min}$. This is another manifestation that T_{\min} is an essential physical parameter, directly reflecting DOS features. The relation

between T_{\min} and the change of the transition order follows from the model of the metamagnetic transition of Co subsystem² as a consequence of the temperature smearing of DOS features at the Fermi level^{2,17}. Essentially the

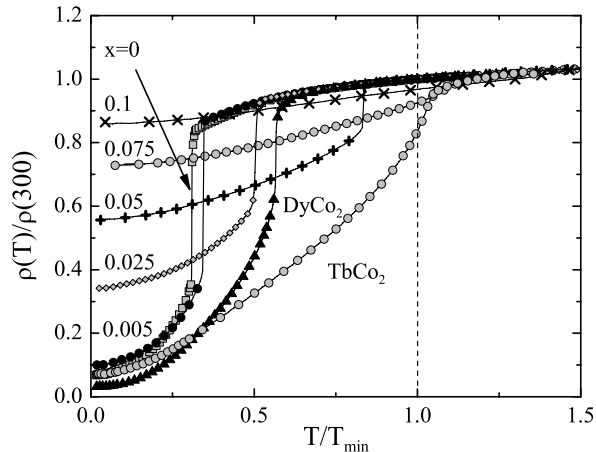


FIG. 6: Normalized resistivity $\rho(T)/\rho(300)$ against normalized temperature T/T_{\min} for $\text{Ho}(\text{Co}_{1-x}\text{Al}_x)_2$ alloys and DyCo_2 , TbCo_2 compounds³⁹.

same mechanism leads to the development of the minima in $S(T)$ ¹². There is, however, an alternative theoretical model, in which the order of a magnetic phase transition depends basically on the lattice constant value⁴⁰. Since the width of the DOS peak (and, therefore, T_{\min}) is determined in pure $R\text{Co}_2$ compounds by the lattice parameter, $T_c/T_{\min} \approx 1$ represents a more general condition for the boundary between second and first order phase transition in these compounds.

2. The magnitude of the resistivity drop at the Curie temperature $\Delta\rho(T_c)$ decreases as T_c approaches T_{\min} . This last feature is also present in binary $R\text{Co}_2$ compounds, as it can be seen comparing the resistivities of HoCo_2 and DyCo_2 , shown in Fig. 6. The resistivity drop at T_c of heavy $R\text{Co}_2$ compounds, which exhibit a first-order transition, has been attributed to a sudden suppression of SF by strong molecular field of the ordered $4f$ moments³. This, however, does not explain the decrease of $\Delta\rho(T_c)$ with increasing T_c . We propose that the origin of this decrease is the same as the origin of resistivity saturation of nearly magnetic compounds at high temperatures^{41,42}. In the model, put forth in^{41,42} by Ueda and Moriya, the SF contribution to the resistivity (ρ_{sf}) is determined by the d band dynamical susceptibility, which is enhanced due to d band SF. It has been shown that the saturation tendency, which is characteristic for the temperature dependent resistivity of nearly magnetic materials, originates from the strong decrease of the d band enhancement owing to interactions among SF at high temperatures.

We use here a very simplified model with a rectangular approximation for the Co $3d$ DOS (Fig. 7) to illustrate the essential physics of the resistivity saturation and of the decrease of $\Delta\rho(T_c)$.

We consider an enhanced $3d$ band paramagnetic compound (such as YCo_2). At $T=0$ K, without external field, the spin-up and spin-down sub-bands are equally occupied, Fig. 7a, and there are no SF. At a nonzero temperature thermal fluctuations of the $3d$ sub-band occupation, amplified by exchange interaction, result in fluctuations of local magnetization, i.e. SF. According to⁴² the magnitude of the local magnetization fluctuations ($\langle m^2 \rangle$)^{1/2} increases with temperature, however it saturates at a constant value in a high temperature limit. Both, the saturation value and cross-over temperature, are determined by the $3d$ band parameters.

In magnetic $R\text{Co}_2$ compounds the $3d$ system at $T=0$ K is in high magnetization state. In the following we consider $3d$ band in this case as fully polarized by the exchange field of ordered $4f$ moments, as it schematically shown in Fig. 7b, with saturation magnetic moment $M_f = 2N\delta_0$. As temperature increases, there will be also temperature-induced fluctuations of the $3d$ magnetization around this polarized state.

For our qualitative model we assume that the SF resistivity is determined by the spin-spin correlation function

$$\langle m(0)m(l) \rangle - \langle m(0) \rangle \langle m(l) \rangle,$$

where $m(0)$ and $m(l)$ are the local $3d$ magnetization at lattice point with coordinates $r = 0$ and $r = l$, respectively, and l is distance of order of conduction electron (s -electron) mean free path. The scattering magnitude of conduction electron by a magnetic fluctuation is proportional to its squared magnitude, measured relative to the local background at a distance of order of conduction electron mean free path. Therefore, the most effective will be the scattering on correlated magnetic fluctuations with largest difference of local magnetization at points $r = 0$ and $r = l$. For the paramagnetic state, this corresponds to fluctuations at $r = 0$ and $r = l$ with the opposite magnetization. While for a system in ferromagnetic ground state with fully polarized $3d$ band, the largest difference is between this fully polarized state moment M_f and local fluctuation with a reduced moment. Basing on the above arguments, we define the effective SF magnitude (m_p - paramagnetic state, m_f - ferromagnetic state), determining the SF resistivity, as:

$$m_p \propto 2(D_{\text{up}} - D_{\text{dn}}), \quad (1)$$

where

$$D_{\text{up(dn)}} = \int_{-(2W - \delta_0 \pm (\mp)\zeta k_B T)}^{\infty} N f^0 d\varepsilon,$$

and

$$m_f \propto M_f - (D_{\text{up}} - D_{\text{dn}}), \quad (2)$$

with

$$D_{\text{up}} = \int_{-(2W - \zeta k_B T)}^{\infty} N f^0 d\varepsilon$$

and

$$D_{\text{dn}} = \int_{-(2W-2\delta_0+\zeta k_B T)}^{\infty} N f^0 d\varepsilon.$$

The definitions of W , δ_0 and N are given in Fig. 7. D_{up} and D_{dn} are local spin-up and spin-down density, f^0 is the Fermi distribution function, and ζ is the exchange enhancement factor.

Due to the charge neutrality condition ($D_{\text{up}} + D_{\text{dn}} = \text{const}$), the magnitude of the SF has an upper limit. Both m_p and m_f have maximum value of $4N\delta_0$. For the unpolarized $3d$ band the SF attain the maximum amplitude at a temperature T_m satisfying condition $\zeta k_B T_m = \delta_0$, whereas for the fully polarized $3d$ band the corresponding condition is $\zeta k_B T_m = 2\delta_0$. At higher temperatures the itinerant SF behave as localized magnetic moments with fixed magnitude.

The corresponding SF resistivity follows from Eqns. 1 and 2:

$$\rho_p \propto (m_p)^2 \propto \begin{cases} (4N\zeta k_B T)^2 & \text{if } T \leq \frac{\delta_0}{\zeta k_B} \\ (4N\delta_0)^2 & \text{if } T > \frac{\delta_0}{\zeta k_B} \end{cases},$$

for the non-polarized (paramagnetic) state, and

$$\rho_f \propto (m_f)^2 \propto \begin{cases} (2N\zeta k_B T)^2 & \text{if } T \leq \frac{2\delta_0}{\zeta k_B} \\ (4N\delta_0)^2 & \text{if } T > \frac{2\delta_0}{\zeta k_B} \end{cases},$$

for the polarized (magnetically ordered) $3d$ band. Expression for ρ_p gives a roughly correct representation of the overall temperature dependence of the SF resistivity of paramagnetic $R\text{Co}_2$ compounds: it increases as T^2 at low temperatures and saturates to a temperature-independent value at high temperatures³. Both, ρ_p and

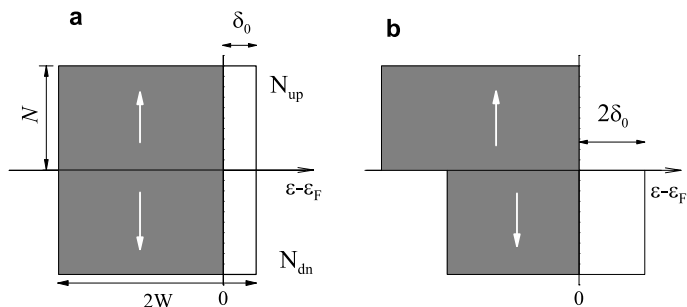


FIG. 7: The model of $3d$ DOS: **a.** Non polarized state at $T=0$ K; **b.** Polarized state at $T=0$ K. $2W$ is the $3d$ band width, δ_0 is the distance from Fermi energy to the top of $3d$ band and N – DOS magnitude.

ρ_f are displayed in Fig. 8. In $R\text{Co}_2$ compounds with a first-order magnetic phase transition, the $3d$ band undergoes at T_c a transition from the non-polarized to the polarized state (shown schematically by the arrows in Fig. 8), with corresponding change of the SF resistivity: $\Delta\rho = \rho_p - \rho_f$, which is also presented in Fig. 8.

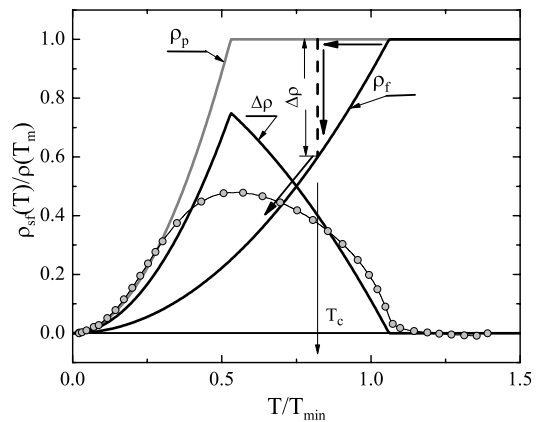


FIG. 8: Schematic temperature dependence of normalized ρ_{sf} for polarized (ρ_f) and non-polarized (ρ_p) states of the $3d$ band and temperature dependence of resistivity jump at first order transition from non-polarized to polarized (ferromagnetic) state $\Delta\rho = \rho_p - \rho_f$. The circles show the experimental difference between the normalized resistivities of paramagnetic YCo_2 and ferrimagnetic TbCo_2 ³⁹. The temperature is normalized to T_{min} of $\text{TbCo}_2 = 214$ K³. $T_m = \frac{2\delta_0}{\zeta k_B}$.

For comparison the experimental difference between the normalized resistivity of paramagnetic YCo_2 ³⁹ (a representative of a non-polarized state of the $3d$ band) and of ferrimagnetic TbCo_2 ³⁹ (a representative of the polarized state of the $3d$ band) is shown on this figure too. In spite of very schematic model, used to calculate $\Delta\rho$, there is close correspondence between theoretical and experimental curve.

The experimental resistivity jump observed at T_c of $R\text{Co}_2$ and $\text{Ho}(\text{Co}_{1-x}\text{Al}_x)_2$ is presented in Fig. 9. $\Delta\rho(T_c)$ is shown for pure TmCo_2 ⁴⁴, ErCo_2 , HoCo_2 , DyCo_2 ³⁹ compounds and for $\text{Ho}(\text{Co}_{1-x}\text{Al}_x)_2$ alloys. Also shown are the results for ErCo_2 , HoCo_2 and DyCo_2 under pressure up to 16 kbar⁴³. The resistivity drop is plotted against T_c/T_{min} to account for the different width of Co- $3d$ band. We do not have experimental data on thermopower of all $R\text{Co}_2$ under pressure, therefore the same value of $\frac{dT_{\text{min}}}{dP} = 0.7$ K/kbar was used to calculate T_{min} for compounds under pressure, shown in Fig. 9. $\frac{dT_{\text{min}}}{dP}$ was obtained experimentally for a $(\text{Gd}_{0.01}\text{Y}_{0.99})\text{Co}_2$ alloy⁴⁵. As it can be seen from the Fig. 9 there is qualitative agreement between theoretical and experimental values of $\Delta\rho$. The model shows two important features in the resistivity behavior: the saturation at high temperatures, and the decrease of $\Delta\rho(T_c)$ with increasing T_c . The important parameters of the model are the bandwidth $2W$ and the distance from the Fermi level to band edge δ_0 . They can be estimated in the following way. The empty portion of the $3d$ band can be evaluated from the experimentally observed saturation Co-moment $M=1 \mu_B/\text{Co}$ for $R\text{Co}_2$ compounds. From this value it follows that $\delta_0 \approx 0.1W$. Using the experimentally observed temperature range in which $\Delta\rho$ is non-zero (Fig. 9) as the measure for δ_0 (200 K), and taking $\zeta = 7$ ²² (which gives

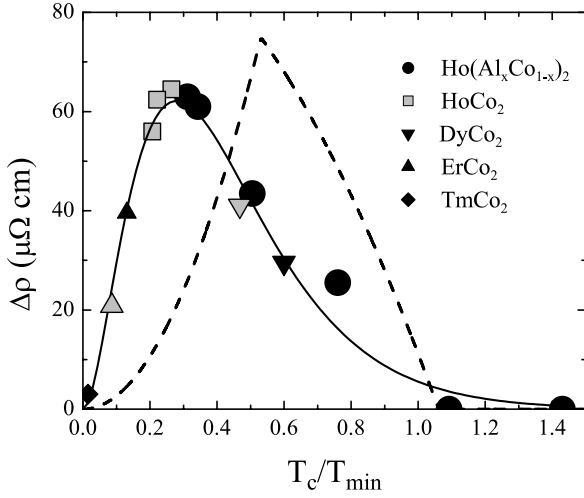


FIG. 9: The resistivity drop $\Delta\rho$ at Curie temperature of $\text{Ho}(\text{Co}_{1-x}\text{Al}_x)_2$ alloys and of some $R\text{Co}_2$ compounds^{39,44}. Broken line is theoretical $\Delta\rho$, scaled with $\rho(T_m)=100 \mu\Omega \text{ cm}$. The gray symbols stand for data under pressure for corresponding compounds⁴³.

$\delta_0 \approx 0.12 \text{ eV}$), we get for Co- $3d$ bandwidth $2W$ about 2.4 eV , in a very reasonable agreement with the value of 2.5 eV , according to the result of Ref.²².

The model DOS used here to demonstrate the mechanism of $\Delta\rho(T_c)$ decrease with increasing T_c , is obviously too oversimplified to account for the very details of $\rho_{\text{sf}}(T)$ and $\Delta\rho(T_c)$. The omission of $4f-3d$ exchange interaction is less obvious. This effect, however, is clearly visible, if one compares $\rho(T)$ of paramagnetic and magnetic $R\text{Co}_2$ compounds, depicted in Fig. 10. For a hy-

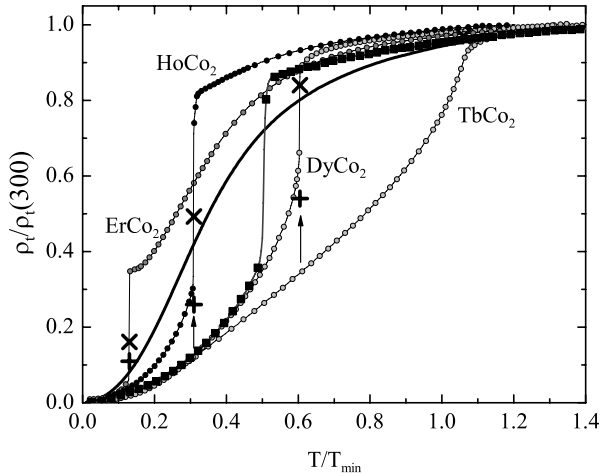


FIG. 10: Normalized resistivity of $R\text{Co}_2$ compounds³⁹ and $\text{Ho}(\text{Co}_{0.975}\text{Al}_{0.025})_2$ alloy (■). The solid line is the resistivity of YCo_2 . $\rho_t = \rho(T) - \rho(4.2)$. 'X' and '+' indicate resistivity at T_c , including corrections for ρ_{spd} and ρ_{sw} in paramagnetic and ferrimagnetic phase, respectively.

pothetical magnetic $R\text{Co}_2$ compound, whose resistivity includes only SF, phonon, and impurity contributions,

its normalized resistivity above T_c would coincide with the normalized resistivity of paramagnetic YCo_2 , while below T_c it should be similar to the normalized resistivity of TbCo_2 . However, as we can see from Fig. 10, the normalized resistivity of the other magnetic $R\text{Co}_2$ compounds deviates on approach to T_c from the resistivity of TbCo_2 at $T < T_c$ and from the resistivity of YCo_2 at $T > T_c$. In part, this deviation refers to additional contributions owing to scattering on $4f$ magnetic moments in magnetic $R\text{Co}_2$. At $T > T_c$, the corresponding contribution, ρ_{spd} , is independent of temperature. Therefore, the normalized resistivity of a magnetic compound:

$$\frac{\rho(T)}{\rho(300)} = \frac{\rho_{\text{YCo}_2}(T) + \rho_{\text{spd}}}{\rho_{\text{YCo}_2}(300) + \rho_{\text{spd}}}$$

differs from the normalized resistivity of YCo_2 .

Below T_c , instead of ρ_{spd} there is a temperature-dependent $4f$ spin-wave contribution to the resistivity, ρ_{sw} . It increases with temperature, reaching at T_c a maximum value. In ferromagnetic metals with second-order phase transition, $\rho_{\text{sw}}(T_c) \approx \rho_{\text{spd}}$, however in $R\text{Co}_2$ with first-order transition it should be strongly suppressed by the $3d$ exchange field just below the transition. The estimated resistivity at T_c , including contributions of ρ_{spd} or ρ_{sw} is shown in Fig. 10. For these estimations we use $\rho_{\text{sw}}(T_c) = \rho_{\text{spd}}$, with ρ_{spd} from Ref.³. Corrections due to ρ_{sw} are certainly overestimated. Nevertheless, it is clear from Fig. 10 that these corrections can not account for the observed deviations, especially above T_c . The origin of these deviations is the mutual interaction between the $4f$ and the $3d$ magnetic systems. Below T_c , the spin-wave excitations in the $4f$ system amplify the itinerant SF of the $3d$ polarized band, leading to strong increase of the resistivity on approaching T_c . In the paramagnetic state there is a similar mutual amplification of $4f$ and $3d$ SF on approach to T_c from higher temperatures. This amplification increases with decreasing T_c since the susceptibility of the localized $4f$ moments increases with decreasing temperature.

C. Thermopower.

$S(T)$ above T_c is related to DOS features in vicinity of the Fermi energy. Results for $\text{Ho}(\text{Co}_{1-x}\text{Al}_x)_2$ alloys provide further support to the model outlined in our previous publications^{12,18}.

We use similar approach and the model DOS, depicted in Fig. 3 by the dotted line, to explore the dependence of the thermopower on Co $3d$ band parameters. According to Mott's $s-d$ model, the conductivity is due to high mobility s -electron states, from which the charge carriers are scattered into $3d$ states with low mobility and, effectively, are eliminated from conduction process. The scattering probability of conduction electrons is proportional to the state density value, into which an electron is scattered. Therefore, within $s-d$ model, the s -electron

scattering probability P is expected to depend on the electron energy as:

$$P(\varepsilon - \varepsilon_F) \propto N_d(\varepsilon - \varepsilon_F) + R \quad (3)$$

where R is due to other than s - d scattering transitions. This relation is valid for elastic or quasi-elastic scattering.

Thermopower is expressed as^{18,46}:

$$S(T) = -\frac{1}{|e|T} \frac{\int_0^\infty \omega(\varepsilon, T) \left(-\frac{\partial f^0}{\partial \varepsilon}\right) (\varepsilon - \varepsilon_F) d\varepsilon}{\sigma(T)}, \quad (4)$$

where

$$\sigma(T) = \int_0^\infty \omega(\varepsilon, T) \left(-\frac{\partial f^0}{\partial \varepsilon}\right) d\varepsilon \quad (5)$$

and

$$\omega(\varepsilon, T) = \frac{e^2}{12\pi^3\hbar} v A(\varepsilon) \tau(\varepsilon, T), \quad (6)$$

where v is the velocity of conduction electrons, $A(\varepsilon)$ is the cross-sectional area of the Fermi surface, perpendicular to the electrical field direction. $\tau \propto \frac{1}{P}$ is the relaxation time. In the s - d model approximation

$$\tau(\varepsilon - \varepsilon_F) \propto \frac{1}{N_d(\varepsilon - \varepsilon_F) + R}. \quad (7)$$

Using equations (4-7) $S(T)$ is calculated with the model DOS, shown in Fig. 3. The results of the calculations are shown in Fig. 11. The calculations were performed using different values of two parameters describing the model DOS: Γ is the width of the $3d$ DOS peak, and Δ - is the distance from Fermi energy to the center of the peak. Two important conclusions follow from these results:

1. The position of the thermopower minimum depends mainly on the $3d$ peak width;
2. The de-population of the $3d$ band affects the magnitude of the high-temperature thermopower, however has almost no effect on the position of the thermopower minimum.

Comparison of the theoretical result of Fig. 11c and experimental data on thermopower (Fig. 2) indicates that both effects - de-population and narrowing of $3d$ band, play an important role determining $S(T)$ in the paramagnetic temperature range. Both also lead to an increase of $3d$ DOS at Fermi level. From the variation of parameters Δ and Γ we can roughly estimate that the narrowing of $3d$ band increases DOS at Fermi level by more than 50%, while de-population - by less than 20%. Therefore, this estimation support our conjecture, that narrowing of $3d$ band due to disorder plays dominant role in the magnetic enhancement of $R(\text{Co}_{1-x}\text{M}_x)_2$ alloys.

The calculations of thermopower were made under assumption of elastic scattering, which is valid at high temperatures, i.e. above about 100 K. At lower temperatures

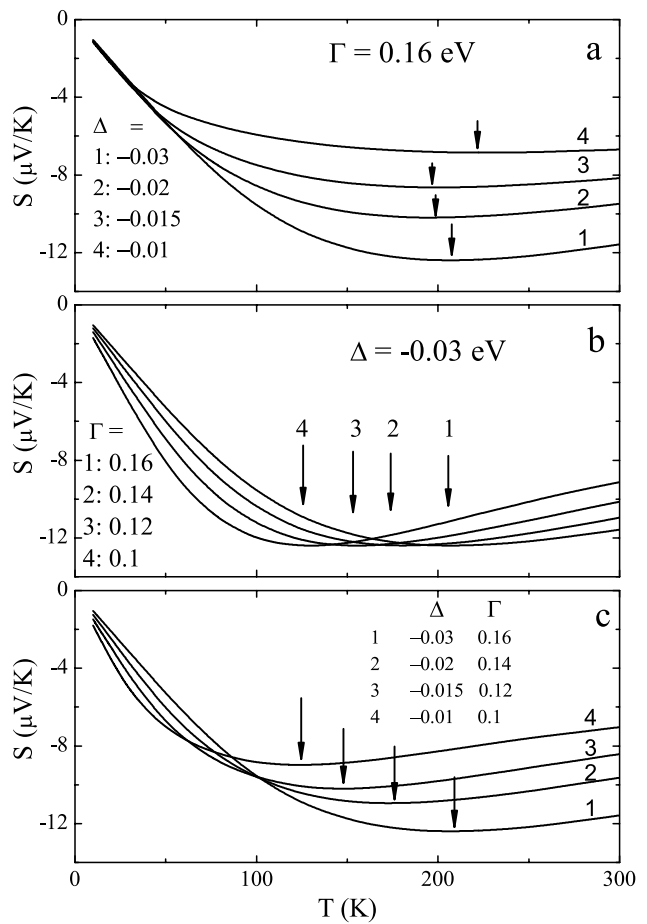


FIG. 11: The temperature dependencies of thermopower calculated within s - d scattering model approximation. **a.** The DOS peak width is fixed at $\Gamma=0.16$ eV, the distance from the Fermi energy to the center of the DOS peak, Δ , varies, simulating the de-population of the $3d$ band. **b.** The occupation of the $3d$ band is fixed at -0.03 eV, the width of the $3d$ peak varies. **c.** Both, Γ and the absolute value of Δ decrease. The arrows indicate position of the thermopower minimum.

scattering on SF is non-elastic. The distinction between elastic and non-elastic scattering is essential in case of thermopower (however it is not important for resistivity). For elastic scattering the change of conduction electron energy satisfies the condition: $|\varepsilon(k') - \varepsilon(k)| \ll k_B T$, where k' and k denote the final and initial states, respectively. In non-elastic scattering the change of the electron energy in a scattering event is of order of $k_B T$. On average, an electron from a state above ε_F will be scattered into a state below ε_F and vice versa. Therefore, while for elastic scattering (due to negative $\frac{dN_d}{d\varepsilon}$ values at Fermi energy) $\tau(\varepsilon > \varepsilon_F) > \tau(\varepsilon < \varepsilon_F)$, for the non-elastic scattering it can be reversed: $\tau(\varepsilon > \varepsilon_F) < \tau(\varepsilon < \varepsilon_F)$, leading to a positive thermopower, instead of negative values for elastic scattering. The effect of these different scattering regimes is clearly visible in $S(T)$ of paramagnetic RCO_2 compounds³: with decreasing temperature below about 100 K $S(T)$ shows a clear tendency to change sign, which,

however, is interrupted by another process, leading to large negative thermopower values at low temperatures. This another process is likely caused by SF drag effect.

$S(T)$ of $\text{Ho}(\text{Co}_{1-x}\text{Al}_x)_2$ at $T < T_c$ exhibits a complicated variation as obvious from Fig. 12. Data imply that

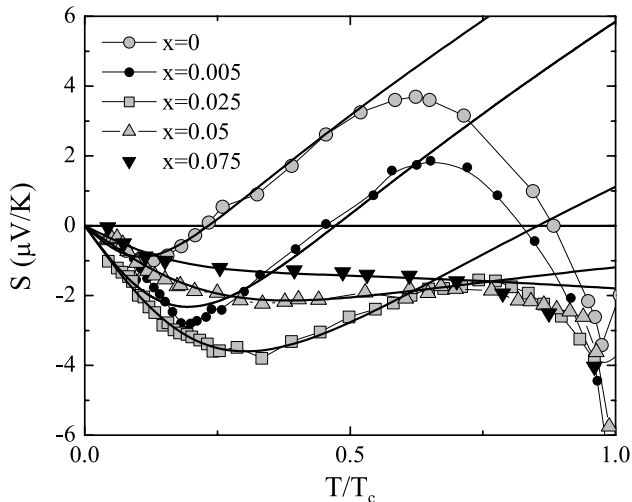


FIG. 12: Low temperature thermopower of $\text{Ho}(\text{Co}_{1-x}\text{Al}_x)_2$. The solid lines represent the Nordheim-Gorter expression (8) with parameters, listed in Table I.

these temperature dependencies result from an interplay between impurity (elastic) and spin wave (non-elastic) scattering. For diluted alloys at low temperatures, the impurity scattering constitutes the main contribution to thermopower. This gives rise to negative $S(T)$ values, exhibiting an almost linear temperature variation. At higher temperatures, non-elastic scattering on spin waves becomes important and results in the pronounced positive peak, especially at lower Al content. According to the Nordheim-Gorter rule⁴⁶, thermopower of a conductor with two dominating scattering processes, can be expressed as:

$$S = \frac{S_0 \rho_0}{\rho} + \frac{S_{\text{sw}} \rho_{\text{sw}}}{\rho},$$

with $\rho = \rho_0 + \rho_{\text{sw}}$. The subscripts refer to impurity and spin-wave scattering contributions. The resistivity related to scattering on spin-waves follows from $\rho_{\text{sw}} = AT^2$. We assume that both, S_0 and S_{sw} , are linear at low temperatures: $S_0 = b_0 T$, and $S_{\text{sw}} = b_{\text{sw}} T$. Based on these assumptions we obtain for the total thermopower:

$$S = \frac{T}{1 + \left(\frac{T}{T_0}\right)^2} \left[b_0 + b_{\text{sw}} \left(\frac{T}{T_0}\right)^2 \right], \quad (8)$$

where T_0 is temperature, defined from the condition:

$$AT_0^2 = \rho_0.$$

Expression (8) was fitted to the low temperature experi-

TABLE I: Fitted parameters of Eqn. 8

x	b_0	b_{sw}	T_0
0	-0.18	0.12	15
0.005	-0.25	0.1	24
0.025	-0.22	0.05	39
0.05	-0.09	0.0037	49
0.075	-0.055	-0.001	40

mental thermopower, using b_0 , b_{sw} and T_0 as free parameters. The results are shown in Fig. 12 by solid lines, and the parameter values are listed in Table I. For diluted alloys ($x=0$, $x=0.005$) the parameters are reasonable and show expected dependencies on x : b_0 and T_0 increase with x , while b_{sw} is independent of x . At larger values of x , however, the dominant low-temperature scattering mechanism is due to static magnetic disorder, related to the formation of a partially-ordered ground state of the $3d$ electron system. This scattering is not temperature independent, which leads to a decrease of b_0 and b_{sw} in concentrated alloys.

IV. CONCLUSION

In conclusion, we have studied electrical resistivity and thermoelectric power of $\text{Ho}(\text{Co}_{1-x}\text{Al}_x)_2$ alloys ($0 \leq x \leq 0.1$) for temperatures from 4.2 K to 300 K. The experimental temperature dependencies of thermopower indicate that the width of the Co $3d$ band decreases with Al content. This decrease can not be accounted for only by the increasing lattice parameter of the alloys. The analysis of experimental results on magnetic and transport properties of $\text{Ho}(\text{Co}_{1-x}\text{Al}_x)_2$ and other $R(\text{Co}_{1-x}M_x)_2$ alloys led us to the conclusion that the principal mechanism, responsible for the narrowing of the $3d$ DOS peak is the localization of the Co $3d$ electron states, induced by disorder in Co sublattice of the alloys. The narrowing of the $3d$ DOS gives main contribution to enhancement of DOS at Fermi energy and to increase of T_c in magnetic alloys, or a decrease of B_c in paramagnetic alloys. This new mechanism of a magnetic enhancement of the Co $3d$ band in $R\text{Co}_2$ -based alloys upon substitution of Co by non-magnetic elements reconciles two previous, apparently conflicting, models.

The magnitude of the resistivity jump at Curie temperature, observable in $\text{Ho}(\text{Co}_{1-x}\text{Al}_x)_2$ and $R\text{Co}_2$ compounds, exhibiting first order magnetic phase transition, is a non-monotonic function of T_c . Our simple model shows that the non-monotonous variation of the resistivity jump with T_c is due to the saturation of the $3d$ band SF magnitude at high temperatures.

We postulate that fluctuations of the local magnetic susceptibility in $\text{Ho}(\text{Co}_{1-x}\text{Al}_x)_2$ leads to development of partially ordered ground state of the $3d$ magnetic subsystem, as it was shown previously for $Y_{1-x}R_x\text{Co}_2$ alloys (R are magnetic rare earth elements). Static magnetic disorder, associated with this partially ordered ground state,

induces the huge residual resistivities observed. With increasing temperature the static magnetic disorder is replaced by dynamic, temperature-induced SF. The corresponding contributions to the resistivity have similar magnitude. Therefore, the overall temperature variation of the resistivity in the alloys is strongly suppressed.

Our analysis demonstrate that the temperature behavior of the thermopower above 100 K is determined by a narrow peak in the $3d$ DOS at the Fermi energy. The complex behavior of the thermopower at low temperatures results from an interplay of elastic impurity scatter-

ing and non-elastic temperature-induced SF scattering.

V. ACKNOWLEDGMENTS

We want to thank Dr. A.Yu.Zyuzin for stimulating discussions.

This work was supported by Russian Foundation for Basic Research under Grants 05-02-17816-a and 06-02-17047-a.

-
- ¹ R. Lemaire, *Cobalt* **32** (1966) 132; **33** 201 (1966).
² R. Z. Levitin, A. S. Markosyan, *Sov. Phys. - Usp.* **31** 730 (1988).
³ E. Gratz, R. Resel, A. T. Burkov, E. Bauer, A. S. Markosyan, A. Galatanu, *J. Phys.: Condens. Matter* **7** 6687 (1995).
⁴ T. Goto, K. Fukamichi, T. Sakakibara, H. Komatsu, *Solid State Commun.* **72** 945 (1989).
⁵ T. Goto, T. Sakakibara, K. Murata, K. Komatsu, K. Fukamichi, *J. Magn. Magn. Mater.* **90/91** 700 (1990).
⁶ V. V. Aleksandryan, A. S. Lagutin, R. Z. Levitin, A. S. Markosyan, V. V. Snegirev, *Sov.Phys.-JETP* **62** 153 (1985).
⁷ K. Yoshimura, Y. Nakamura, *Solid State Commun.* **56** 767 (1985).
⁸ V. V. Aleksandryan, K. P. Belov, R. Z. Levitin, A. S. Markosyan, V. V. Snegirev, *JETP Letters* **40** 815 (1984).
⁹ R. Ballou, Z. M. Gamishidze, R. Lemaire, R. Z. Levitin, A. S. Markosyan, V. V. Snegirev, *Sov. Phys. JETP* **75** 1041 (1993).
¹⁰ K. Ishiyama, K. Endo, *J. Phys. Soc. Japan* **55** 2535 (1986).
¹¹ This DOS feature is responsible for the itinerant metamagnetism of $R\text{Co}_2$ compounds.
¹² A. T. Burkov, M. V. Vedernikov, E. Gratz, *Solid State Commun.* **67** 1109 (1988).
¹³ M. Forker, S. Müller, P. de la Presa, A. F. Pasquevich, *Phys. Rev. B* **68** 014409 (2003).
¹⁴ M. Forker, S. Müller, P. de la Presa, A. F. Pasquevich, *Phys. Rev. B* **75** 187401 (2007).
¹⁵ J. Herrero-Albillos, F. Bartolomè, L. M. García, F. Casanova, A. Labarta, X. Batlle, *Phys. Rev. B* **73** 134410 (2006).
¹⁶ J. Herrero-Albillos, F. Bartolomè, L. M. García, F. Casanova, A. Labarta, X. Batlle, *Phys. Rev. B* **75** 187402 (2007).
¹⁷ N. H. Duc, T. D. Hien, R. Z. Levitin, A. S. Markosyan, P. E. Brommer, J. J. M. Franse, *Physica B* **176** 232 (1992).
¹⁸ A. T. Burkov, E. Gratz, E. Bauer, R. Resel, *J. Alloys Compd.* **198** 117 (1993).
¹⁹ M. Cyrot, M. Lavagna, *J.Physique* **40** 763 (1979).
²⁰ H. Yamada, J. Inoue, K. Terao, S. Kanda, M. Shimizu, *J. Phys. F: Metal Physics* **14** 1943 (1984).
²¹ H. Yamada, *Physica B* **149** 390 (1988).
²² S. Tanaka and H. Harima, *J. Phys. Soc. Japan* **67** 2594 (1998).
²³ N. H. Duc, T. K. Oanh, *J. Phys.: Condens. Matter* **9** 1585 (1997).
²⁴ K. Murata, K. Fukamichi, H. Komatsu, T. Sakakibara, T. Goto, *J. Phys.: Condens. Matter* **3** 2515 (1991).
²⁵ K. Murata, K. Fukamichi, T. Sakakibara, T. Goto, K. Suzuki, *J. Phys.: Condens. Matter* **5** 1525 (1993).
²⁶ D. Michels, J. Timlin, T. Mihhlisin, *J. Appl. Phys.* **67** 5289 (1990).
²⁷ H. Wada, M. Hada, K. N. Ishihara, M. Shiga, Y. Nakamura, *J. Phys. Soc. Japan* **59** 2956 (1990).
²⁸ I. L. Gabelko, R. Z. Levitin, A. S. Markosyan, V. I. Silantiev, V. V. Snegirev, *J. Magn. Magn. Mater.* **94** 287 (1991).
²⁹ T. Nakama, K. Shintani, M. Hedo, H. Niki, A. T. Burkov, K. Yagasaki, *Physica B* **281&282** 699 (2000).
³⁰ T. Goto, H. Aruga Katori, T. Mitamura, K. Fukamichi, K. Murata, *J. Appl. Phys.* **76** 6682 (1994).
³¹ W. Steiner, E. Gratz, H. Ortbauer, H. W. Gamen, *J.Phys. F: Metal Physics* **8** 1525 (1978).
³² E. Gratz, N. Pillmayr, E. Bauer, , G. Hilscher, *J. Magn. Magn. Mater.* **70** 159 (1987).
³³ N. H. Duc, V. Sechovski, D. T. Hung, N. H. K. Ngan, *Physica B* **179** 111 (1992).
³⁴ N. H. Duc, P. E. Brommer, X. Li, F. R. de Boer, J. J. M. Franse, *Physica B* **212** 83 (1995).
³⁵ E. Gratz, R. Hauser, A. Lindbaum, M. Maikis, R. Resel, G. Schaudy, R. Z. Levitin, A. S. Markosyan, I. S. Dubenko, A. Yu. Sokolov, S. W. Zochowski, *J.Phys.: Condens. Matter* **7** 597 (1995).
³⁶ N. V. Baranov, A. N. Pirogov, *J. Alloys Compd.* **217** 31 (1995).
³⁷ N. V. Baranov, A. A. Yermakov, A. Podlesnyak, *J. Phys.: Condens. Matter* **15** 5371 (2003).
³⁸ A. T. Burkov, A. Yu. Zyuzin, T. Nakama, K. Yagasaki, *Phys. Rev. B* **69** 144409 (2004).
³⁹ We measured resistivity of pure $R\text{Co}_2$ compounds (except TmCo_2) using new samples, prepared according to the same procedure as the samples of $\text{Ho}(\text{Al}_x\text{Co}_{1-x})$ alloys. These new results agree within experimental uncertainty with earlier data from Refs.^{3,43}.
⁴⁰ S. Khmelevskiy, P. Mohn, *J. Phys.: Condens. Matter* **12** 9453 (2000).
⁴¹ K. Ueda, T. Moriya, *J. Phys. Soc. Japan* **39** 605 (1975).
⁴² T. Moriya, *Spin Fluctuations in Itinerant Electron Magnetism*. Springer Series in Solid State Sciences **56**, Ed. M. Cardona, P. Fulde, H.-J. Quisser. Springer-Verlag, Berlin, Heidelberg, 1985.
⁴³ R. Hauser, E. Bauer, E. Gratz, *Phys. Rev. B* **57** 2904 (1998).

- ⁴⁴ T. Nakama, K. Shintani, K. Yagasaki, A. T. Burkov, Y. Uwatoko, Phys. Rev. B **60**, 511 (1999).
- ⁴⁵ T. Nakama, et al., unpublished.
- ⁴⁶ R. D. Barnard, *Thermoelectricity in metals and alloys*, London: Taylor & Frances, 1972.